View metadata, citation and similar papers at core.ac.uk

brought to you by CORE

provided by University of Lincoln Institutional Repository

Microelectronic Engineering 109 (2013) 68–71

Contents lists available at SciVerse ScienceDirect

Microelectronic Engineering

journal homepage: www.elsevier.com/locate/mee

Identification of intrinsic electron trapping sites in bulk amorphous silica from *ab initio* calculations

Al-Moatasem El-Sayed [a,*], Matthew B. Watkins [a], Alexander L. Shluger [a], Valeri V. Afanas'ev [b]

[a] Department of Physics and Astronomy and London Centre for Nanotechnology, University College London, Gower Street, London WC1E 6BT, United Kingdom
[b] Department of Physics, University of Leuven, Celestijnenlaan 200D, 3001 Leuven, Belgium

ARTICLE INFO

Article history:
Available online 18 March 2013

Keywords:
Silica defects
Electron trapping
Device Reliability
Deep state traps

ABSTRACT

Using *ab initio* calculations we demonstrate that extra electrons in pure amorphous SiO_2 can be trapped in deep band gap states. Classical potentials were used to generate amorphous silica models and density functional theory to characterise the geometrical and electronic structures of trapped electrons. Extra electrons can trap spontaneously on pre-existing structural precursors in amorphous SiO_2 and produce ≈3.2 eV deep states in the band gap. These precursors comprise wide (⩾130°) O–Si–O angles and elongated Si–O bonds at the tails of corresponding distributions. The electron trapping in amorphous silica structure results in an opening of the O–Si–O angle (up to almost 180°). We estimate the concentration of these electron trapping sites to be $\approx 5 \times 10^{19}$ cm^{-3}.

© 2013 Elsevier B.V. Open access under CC BY license.

1. Introduction

Electron trapping is known to have a dramatic effect on the performance and reliability of electronic devices employing SiO_2 as gate insulator, providing a direct contribution to the electric field at the surface of the semiconductor channel [1]. So far, the dominant electron traps have been associated with impurity-related centres, in particular, the hydrogen-related network fragments [2–5]. However, little is still known regarding the possibility of *intrinsic* electron trapping in the a-SiO_2 network.

Our work stems from as yet unexplained electron trapping observed in device-grade oxides at an energy of 2.8 eV below the conduction band of a-SiO_2. These traps have initially been exposed using photon-stimulated tunnelling experiments on oxidised Si and SiC crystals [6–9]. Additional low-temperature capacitance [10] and Hall effect measurements [11,12] on 4H-SiC MOS devices revealed that the density of these electron trapping states can be as high as 10^{14} cm^{-2} eV^{-1}, with the measured trap density of 10^{13} cm^{-2} inside a 2-nm thick near-interface SiO_2 layer [6,9] corresponding to $\approx 5 \times 10^{19}$ cm^{-3} in terms of volume concentration. Notably, none of the established defects have such a high density in thermally grown a-SiO_2. Several features, including the absence of a comparable density of electron traps in bulk a-SiO_2 and strong sensitivity of electron trapping to the incorporation of nitrogen at the interface [13,14] suggest that electron trapping at 2.8 eV deep centres can be taking place in the near interfacial oxide network.

It has initially been suggested that these electron traps above the conduction band of silicon substrate crystals are correlated with oxygen deficiencies at the near-interfacial oxide [7,8,14]. However, later experiments on nitrided SiC/SiO_2 samples make this link less obvious, particularly when taking into account the fact that the density of known O-deficiency centres (E′ centres, E'_δ centres) rarely approaches the density range of 10^{13} cm^{-2} found for the 2.8 eV deep electron traps. It is more likely that in O-deficient oxides these electron traps may be efficiently filled by electron tunnelling from the substrate while their density is not determined by the O-deficiency *per se*.

There have been suggestions that electrons can be trapped in the bulk and at surfaces of silica [15] but new models of electron trapping centres started to appear only recently. It has been suggested by Bersuker et al., who used molecular models, that electrons can be trapped by Si–O bonds in a-SiO_2 leading to their weakening and thus facilitating Si–O bond dissociation [16]. Further calculations by Camellone et al. have shown that electrons can spontaneously trap in non-defective continuum random network model of a-SiO_2 [17]. Recent calculations have also demonstrated that the two dominant neutral paramagnetic defects at surfaces of a-SiO_2, the non-bridging oxygen centre and the silicon dangling bond, are deep electron traps and can form the corresponding negatively charged defects [18]. However, these theoretical predictions have not yet been confirmed experimentally, emphasising the challenges for identifying defect centres.

In this paper we demonstrate that electrons can be trapped even in an idealised a-SiO_2 matrix forming deep electron states

* Corresponding author. Tel.: +44 (0) 207 3679 7875.
E-mail addresses: al-moatasem.el-sayed.10@ucl.ac.uk (A.-M. El-Sayed), Valeri.Afanasiev@fys.kuleuven.be (V.V. Afanas'ev).
URL: http://www.cmmp.ucl.ac.uk/~kpm/ (A.L. Shluger).

0167-9317© 2013 Elsevier B.V. Open access under CC BY license.
http://dx.doi.org/10.1016/j.mee.2013.03.027

in the gap. These states are not dissimilar to electrons trapped by Ge impurities in α-quartz [19], where the key to the electron trapping is the wide opening of the O–Ge–O angle. It turns out that the precursor sites with wide enough O–Si–O angles present in a-SiO_2 structure facilitate spontaneous electron trapping at these sites. We identify a structural *fingerprint* for these electron trapping sites and use it to estimate the concentration of these sites in a-SiO_2.

2. Details of calculation

The calculations presented in this work make use of both classical force-fields and *ab initio* theory. The ReaxFF [20] force-field was used to generate 20 models of amorphous SiO_2 containing 216 atoms. ReaxFF was parameterised to reproduce the properties of various silica polymorphs, small silica clusters and silicon polymorphs. It allows the calculation of silicon atoms (and oxygen atoms) in varying oxidation states based on the instantaneous geometry. This is accomplished by assigning a charge dependent atomic energy and exploiting the electronegativity equalisation principle [21]. The more extended silica structures, containing between 8,640 to 401,760 atoms were generated using the BKS potential, which is a Buckingham potential parametrised for SiO_2 [22]. All the simulations using ReaxFF were performed using the LAMMPS code [23] and the parameters published by Fogarty et al. [24].

To generate amorphous structures, molecular dynamics simulations were run using ReaxFF and BKS to melt and quench crystalline SiO_2 structures into an amorphous state in a manner similar to previous calculations [25–27]. Starting from supercells with a β-cristobalite structure, the system was equilibrated at 300 K and pressure of 1 atm. Maintaining the pressure at 1 atm, the temperature was linearly ramped to 5000 K (for the ReaxFF simulations) or 7000 K (for the BKS simulations). The temperature was maintained at 5000 K/7000 K for 40 ps and then brought down to 0 K at a rate of 8 K/ps. The resulting structure was then characterised by calculating basic geometrical properties, such as bond lengths, bond angles, density and total structure factor. The peaks calculated for the total structure factor appear at 1.61 Å, 2.63 Å and 3.08 Å, in good agreement with the experimental data [28].

Density functional theory (DFT), implemented in the CP2K code [29], was used to further optimise geometries of these structures and calculate their electronic structures. The HSE functional [30] was used to describe exchange and correlation. The CP2K code uses a mixed Gaussian/plane-wave basis set [31]. The Gaussian basis set employed for all atoms was a double-ζ basis set [32] in conjunction with the GTH pseudopotential [33]. The plane wave cut-off was set to 5440 eV. The exception to this was for the calculation of hyperfine interactions, where the basis sets with contraction schemes (8831/831/1), (8411/411/11) were used for silicon [34] and oxygen [35], respectively. All geometry optimisations were performed to minimise forces on atoms to within 37 pN.

3. Electron trapping in amorphous SiO_2

Amorphous silica structures obtained using the ReaxFF force-field, as described in Section 2, were further optimised at the DFT level. The electronic structure of the systems was calculated and an average band gap of 8.9 eV was obtained. The lowest unoccupied molecular orbital (LUMO) of one of these systems is shown in Fig. 1 clearly indicating that this state is not completely delocalised over the entire system, but is rather localised over the longest Si–O bonds in the system.

An extra electron added to the system occupies the LUMO of the neutral system, i.e. the localised state shown in Fig. 1. The energy minimisation with respect to nuclear coordinates causes a strong

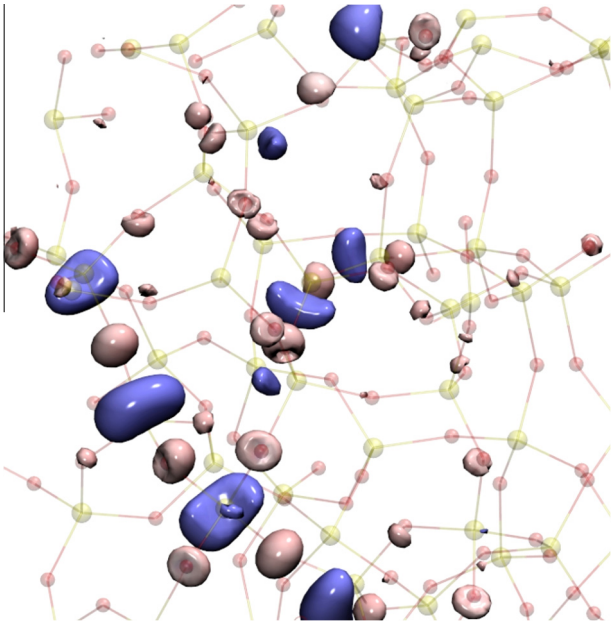

Fig. 1. Visualisation of lowest unoccupied orbital in amorphous SiO_2. The yellow spheres connected to four atoms are Si atoms and the red spheres connected to two atoms are O atoms. The blue and pink shapes are the wavefunction with the 2 colours signifying 2 different phases.

structural distortion around a single SiO_4 tetrahedron shown in Fig. 2. The two Si–O bonds extend from 1.63 Å and 1.64 Å to 1.78 Å and 1.82 Å, respectively. The Si–O–Si angle between these two bonds widens from 125.31° to 172.85°. The remaining two Si–O bonds extend symmetrically from 1.63 Å to 1.70 Å. The resulting energy gain of 3.51 eV indicates that the optimised structure is very stable. The spin density plot in Fig. 2 shows the electron localised into this wide angle. As the electron localises onto the Si atom, it repels the neighbouring oxygen atoms until the O–Si–O angle becomes almost flat.

The electronic structure of this system exhibits a state located below the SiO_2 conduction band minimum (CBM). The average position of this state, from the 20 models, is ≈3.17 eV below the SiO_2

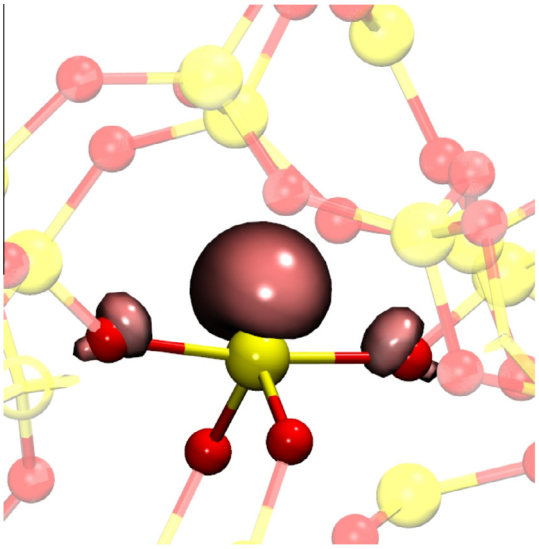

Fig. 2. Visualisation of coordinates of SiO_4 tetrahedron showing spin density of trapped electron.

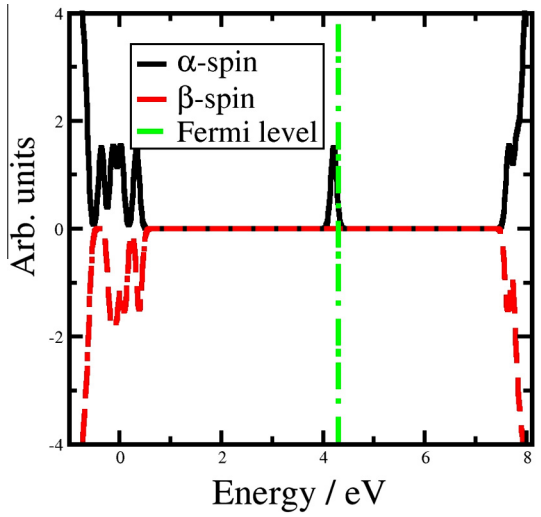

Fig. 3. Electronic density of states of a-SiO_2 with a trapped electron. The extra electron occupies a state at ≈3.2 eV below the bottom of the SiO_2 conduction band.

Table 1
Principal hyperfine values of electron trap in a-SiO_2. Experimental hyperfine interactions for the E′ are shown for comparison. The bond lengths shown are with respect to the Si atom on which the electron is trapped.

Signal	Bond length/Å	Values/mT	Exp./mT [36]
A_{strong} Si		−50.98	−45.31
		−45.45	−39.07
		−45.23	−39.06
O	1.82	−4.181	−0.983
		−2.660	−0.795
		−2.624	−0.791
O	1.78	−5.714	−0.956
		−4.357	−0.751
		−4.298	−0.768
O	1.70	−1.548	
		−1.216	
		−1.212	
O	1.70	−1.581	
		−1.264	
		−1.259	

CBM and ranges from 3.12 eV to 3.21 eV below the CBM. The electronic density of states of one of the SiO_2 systems in which an electron traps is shown in Fig. 3 indicating that this is a deep electron trap. This state is the highest occupied molecular orbital (HOMO) and is mostly localised on the Si atom belonging to the open O–Si–O angle. Calculation of the Mulliken charge difference between the systems where the electron is just added and after the structural relaxation shows that the Si atom trapping the electron becomes more negatively charged by 0.24 eV.

The calculated values of the hyperfine splitting induced by this electron trap are shown in Table 1. The strongest hyperfine interaction is with the Si atom, however, there is a significant interaction with the nearby oxygen atoms. Interestingly, some of the hyperfine interaction values are similar to those for the E′ centre in amorphous silica. This is not surprising considering the strong electron localisation on one Si atom.

Further analysis of the geometric properties of this electron trap in 19 other a-SiO_2 samples reveals that the O–Si–O angle on which the electron traps is the widest initial O–Si–O angle in the sample. Of the 20 models containing 216 atoms of SiO_2, only 4 contained sited which trapped an extra electron. The geometrical properties of amorphous silica are distributions and the extremes of these distributions make up the extremes of the electronic bands. The bottom of the a-SiO_2 conduction band is determined by these extremes of geometrical properties, which lead to localised Anderson-like states forming at the edge of the conduction band [37]. To investigate this point further, we introduced perturbations in our amorphous silica sample to make two other random O–Si–O angles the widest in two separate systems. One angle in one system was changed from 120.3° to 132.1°. An extra electron added into this system localised on the Si on which the angle was changed and caused the O–Si–O angle to open to 160.68°. Another angle in a separate system was changed from 121.3° to 132.0°. When the electron was added to this system, the O–Si–O angle opened to 164.5°. These results demonstrate that a wide O–Si–O bond angle serves as a very efficient precursor to electron trapping in amorphous silica. Further calculations indicate that creating a precursor fluctuation (i.e. opening an O–Si–O angle from an average value of 120° to ≈133°) requires less than 0.5 eV and is within the reach of thermal fluctuations.

The widest existing O–Si–O angle provides a fingerprint for estimating the concentration of such sites in a typical a-SiO_2 sample by analysing its structure. By analysing the twenty models of a-SiO_2 we have determined that the presence of O–Si–O angle exceeding 132°, always leads to spontaneous localisation of extra electrons in a-SiO_2. This angle is at the tail of the O–Si–O angle distribution in regular SiO_2 structures. We then constructed three samples of amorphous SiO_2, as described in Section 2, corresponding to typical device dimensions: 1: $50 \times 25 \times 5\ nm^3$, 2: $25 \times 12.5 \times 2.5\ nm^3$, and 3: $12.5 \times 7 \times 1.5\ nm^3$. These samples included (401,760), (55,296) and 8,640 atoms, respectively. We searched these models for O–Si–O angles above the critical value to estimate the concentration of pre-existing electron trapping precursor sites. Remarkably, in spite of the difference in size and preparation, the concentration of electron trapping sites in all a-SiO_2 models proved to be the same and equal to $\approx 4 \times 10^{19}\ cm^{-3}$.

4. Discussion and conclusions

Our calculations show that intrinsic Si sites with wide O–Si–O bond angles in a-SiO_2 can trap electrons. These electrons localise on Si atoms with an energy ≈3.2 eV below the bottom of the SiO_2 conduction band. The estimated concentration of these electron trapping sites is $\approx 5 \times 10^{19}\ cm^{-3}$. We correlate these states to electron trapping properties identified experimentally in MOS devices [38]. As has been demonstrated experimentally, tunnelling from Si or SiC substrates can be used to fill electron traps which lie 2.8 eV below the bottom of the SiO_2 conduction band. The density of these states is much too high to be attributed to defects which we know about. These electron traps are especially pronounced in 4H–SiC/SiO_2 devices however, they seem to play a role in all devices containing SiO_2 as the dielectric insulating material. For instance, these traps are expected to appear below conduction band of Si nanocrystals in the case of quantum confinement [39]. The concentration of the calculated electron traps approaches the experimentally observed value for the states filled by direct tunnelling. Populating such a density of electron traps via electron injection from an electrode through the SiO_2 conduction band is inefficient because it requires dissipating about 3.5 eV of the relaxation energy into phonons during the trapping process. This process is much less efficient than electron transfer to an opposite electrode.

Acknowledgement

The authors acknowledge EPSRC and the EU FP7 project MORDRED (EU Project Grant No. 261868) for financial support. We

are grateful to G. Bersuker, A. Stesmans, T. Grasser, B. Kaczer, F. Schanovsky and W. Gös for useful discussions. We would like to thank the UK's HPC Materials Chemistry Consortium, which is funded by EPSRC (EP/F067496), via our membership of the UK's HPC Materials Chemistry Consortium, which is funded by EPSRC (EP/F067496), this work made use of the facilities of HECToR, the UK's national high-performance computing service, which is provided by UoE HPCx Ltd at the University of Edinburgh, Cray Inc. and NAG Ltd, and funded by the Office of Science and Technology through EPSRC's High End Computing Programme.

References

[1] D.M. Fleetwood, S.T. Pantelides, R.D. Schrimpf, Defects in Microelecronic Materials and Devices, CRC Press, 2000.
[2] E.H. Nicollian, C.N. Berglund, P.F. Schmidt, J.M. Andrews, J. Appl. Phys. 42 (1971) 5654–5664.
[3] A. Hartstein, D.R. Young, Appl. Phys. Lett. 38 (1981) 631–633.
[4] V.V. Afanas'ev, J.M.M. de Nijs, P. Balk, A. Stesmans, J. Appl. Phys. 78 (1995) 6481–6490.
[5] V.V. Afanas'ev, A. Stesmans, Appl. Phys. Lett. 71 (1997) 3844–3846.
[6] V.V. Afanas'ev, A. Stesmans, Phys. Rev. Lett. 78 (1997) 2437.
[7] V.V. Afanas'ev, A. Stesmans, Appl. Phys. Lett. 70 (1997) 1260.
[8] V.V. Afanas'ev, A. Stesmans, Microelectron. Eng. 36 (1997) 149.
[9] V.V. Afanas'ev, A. Stesmans, J. Phys.: Condens. Matter 9 (1997) L55.
[10] V.V. Afanas'ev, A. Stesmans, M. Bassler, G. Pensl, M.J. Schulz, Appl. Phys. Lett. 76 (2000) 336–338.
[11] N.S. Saks, A.K. Agarwal, Appl. Phys. Lett. 77 (2000) 3281–3283.
[12] N.S. Saks, S.S. Mani, A.K. Agarwal, Appl. Phys. Lett. 76 (2000) 2250–2252.
[13] V.V. Afanas'ev, A. Stesmans, F. Ciobanu, G. Pensl, K.Y. Cheong, S. Dimitrijev, Appl. Phys. Lett. 82 (2003) 568–570.
[14] V.V. Afanasev, F. Ciobanu, S. Dimitrijev, G. Pensl, A. Stesmans, J. Phys.: Condens. Matter 16 (2004) S1839.
[15] A. Takeuchi, H. Nagahama, T. Hashimoto, Phys. Chem. Earth 29 (2004) 359.
[16] G. Bersuker, A. Korkin, Y. Jeon, H. Huff, Appl. Phys. Lett. 80 (2002) 832.
[17] M.F. Camellone, J.C. Reiner, U. Sennhauser, L. Schlapbach, Phys. Rev. B 76 (2007) 125205.
[18] L. Giordano, P.V. Sushko, G. Pacchioni, A.L. Shluger, Phys. Rev. Lett. 99 (2007).
[19] G. Pacchioni, C. Mazzeo, Phys. Rev. B 62 (2000) 5452.
[20] A.C.T. van Duin, A. Strachan, S. Stewman, Q. Zhang, X. Xu, W. Goddard, J. Phys. Chem. A 107 (2003) 3803–3811.
[21] R.T. Sanderson, Chemical Bonds and Bond Energy, Academic Press, 1971.
[22] B.W.H. van Beest, G.J. Kramer, R.A. van Santen, Phys. Rev. Lett. 64 (1990) 1955–1958.
[23] S. Plimpton, J. Comput. Phys. 117 (1995) 1–19.
[24] J.C. Fogarty, H.M. Aktulga, A.Y. Grama, A.C.T. van Duin, S.A. Pandit, J. Chem. Phys. 132 (2010) 174704.
[25] S. Mukhopadhyay, P.V. Sushko, A.M. Stoneham, A.L. Shluger, Phys. Rev. B 70 (2004) 195203.
[26] A. Roder, W. Kob, K. Binder, J. Chem. Phys. 114 (2001) 7602–7614.
[27] K. Vollmayr, W. Kob, K. Binder, Phys. Rev. B 54 (1996) 15808–15827.
[28] S. Susman, K.J. Volin, D.L. Price, M. Grimsditch, J.P. Ringo, R.K. Kalia, P. Vashishta, G. Gwanmesia, Y. Wang, R.C. Liebermann, Phys. Rev. B 43 (1991) 1194.
[29] J. VandeVondele, M. Krack, F. Mohamed, M. Parrinelo, T. Chassaing, J. Hutter, Comput. Phys. Commun. 167 (2005) 103.
[30] J. Heyd, G.E. Scuseria, M. Ernzerhof, J. Chem. Phys. 124 (2006) 219906.
[31] G. Lippert, J. Hutter, M. Parrinello, Mol. Phys. 92 (1997) 477–487.
[32] J. VandeVondele, J. Hutter, J. Chem. Phys. 127 (2007) 114105.
[33] S. Goedecker, M. Teter, J. Hutter, Phys. Rev. B 54 (1996) 1703–1710.
[34] B. Civalleri, P. Ugliengo, J. Phys. Chem. B 104 (2000) 519–532.
[35] M.D. Towler, N.L. Allan, N.M. Harrison, V.R. Saunders, W.C. Mackrodt, E. Apra, Phys. Rev. B 50 (1994) 5041–5054.
[36] M.G. Jani, R.B. Bossoli, L.E. Halliburton, Phys. Rev. B 27 (1983) 2285.
[37] P.W. Anderson, Phys. Rev. 109 (1958) 1492–1505.
[38] I. Pintilie, C.M. Teodorescu, F. Moscatelli, R. Nipoti, A. Poggi, S. Solmi, L.S.L. vlie, B.G. Svensson, J. Appl. Phys. 108 (2010) 024503.
[39] G. Seguini, S. Schamm-Chardon, P. Pellegrino, M. Perego, Appl. Phys. Lett. 99 (2011) 082107.